Highlight

# The NOAA/NASA Pathfinder AVHRR 8-Km Land Data Set

Peter M. Smith,[1] Satya N. V. Kalluri,[2] Steven D. Prince,[2] and Ruth DeFries[2]

## Introduction

The Goddard Space Flight Center's (GSFC) Distributed Active Archive Center (DAAC) has generated a global, long-term (1981-1994) remotely sensed land data set, using measurements from the five-channel, Advanced Very High Resolution Radiometer (AVHRR) instrument (Kidwell, 1991) flown on the NOAA -7, -9 and -11 afternoon orbit satellites. Products from this data set are available free-of-charge to the public and are provided in a variety of formats at spatial resolutions of 8-km and 1°x1°. Generation of this Pathfinder AVHRR Land (PAL) data set is a joint NOAA and NASA activity; NOAA is responsible for providing the raw AVHRR 4-km Global Area Coverage (GAC) data and NASA is responsible for processing, quality checking, archiving, and distributing the data set products (James and Kalluri, 1994). A Land Science Working Group (LSWG) of scientists, chaired by Dr. J. R. G. Townshend of the Department of Geography, University of Maryland, defined the algorithms and validation procedures for the generation of the data set.

## Why is another coarse resolution, vegetation data set needed?

A number of vegetation data sets were generated previously from the AVHRR instrument using different processing schemes. These data sets include the NOAA Global Vegetation Index (GVI) data set, the Global Inventory Monitoring and Modeling System's (GIMMS) continental data, the modified GVI data set, and the 1-km global land data set. All of these data sets have been produced at varying spatial and temporal resolutions, as well as in different map projections. Townshend (1994) has reviewed these data sets. The Earth science community recognized the need for a consistently processed and calibrated, long-term global data set. The Pathfinder AVHRR land project attempts to produce such a data set for global change research, and builds on the valuable lessons learned from the processing experiences of these previous AVHRR data sets. The experience gained in generating the PAL data set will be of considerable value to the upcoming Earth Observing System (EOS) mission (Asrar and Greenstone, 1995).

**Table 1. Pathfinder AVHRR 8-km land data set parameters.**

| | Parameter | Units | Geophysical Minimum Value | Geophysical Maximum Value | Quantization |
|---|---|---|---|---|---|
| 1 | NDVI | - | -1 | 1 | 8 bit |
| 2 | CLAVR Flag | - | 0 | 31 | 8 bit |
| 3 | QC Flag | - | 0 | 31 | 8 bit |
| 4 | Scan Angle | radians | -1.0472 | 1.0472 | 16 bit |
| 5 | Solar Zenith | radians | 0 | 1.3963 | 16 bit |
| 6 | Relative Azimuth | radians | 0 | 6.2832 | 16 bit |
| 7 | Ch1 Reflectance | % | 0 | 100 | 16 bit |
| 8 | Ch2 Reflectance | % | 0 | 100 | 16 bit |
| 9 | Ch3 Btemp | Kelvin | 160 | 340 | 16 bit |
| 10 | Ch4 Btemp | Kelvin | 160 | 340 | 16 bit |
| 11 | Ch5 Btemp | Kelvin | 160 | 340 | 16 bit |
| 12 | Day of Year | DDD.HH | 001.00 | 366.23 | 16 bit |

## Overview of the PAL data set

All data products have been generated using an invariant, community consensus algorithm, enabling this data set to be used as a historical record to study global change. The PAL parameters are listed in Table 1 and are generated at a spatial resolution of 8 km. They are archived as daily and 10-day composite global grids. The parameters may be divided into three main groups: Calibrated reflectances and brightness temperatures from all the 5 bands of AVHRR; the Normalized Difference Vegetation Index (NDVI); and Sun and sensor geometry. Besides these parameters, an experimental cloud condition index (Stowe *et al.*, 1991), quality flags, and time also were provided for each pixel.

NDVI is computed from the visible-red (580-680 nm) and near-IR (725-1100 nm) reflectances from AVHRR channel 1 ($R_1$) and channel 2 ($R_2$), [$NDVI = (R_2-R_1)/(R_2+R_1)$]. The strong correlation of NDVI with vegetation characteristics is due to the near-IR radiation being strongly reflected by vegetation, while the visible-red radiation is strongly absorbed. NDVI has a theoretical dynamic range of -1 to +1. Over land, NDVI increases with vegetation density and green leaf area index, and typical ground observations show NDVI values in the 0. 8 to 0. 9 range for forests (Goward *et al.*, 1994). Bare soils have an NDVI close to zero.

## Major processing features

- Original GAC data has been renavigated and pixel location was determined using an orbital model (Baldwin and Emery, 1993) and a closed form geolocation model (Patt and Gregg, 1994). Geolocation is considered to be accurate to ± one pixel.
- Radiances from the three AVHRR instruments were recalibrated to correct for post-launch instrument degradation (Rao and Chen, 1994; Rao, 1993). Measurements from the three AVHRR instruments flown, on the NOAA -7, -9, and -11 satellites, were normalized to a common baseline defined by the NOAA -9 AVHRR instrument.
- Visible and near IR reflectances have been corrected for the atmospheric effects due to Rayleigh scattering and Ozone absorption (Gordon *et al.*, 1988).
- Ten-day maximum value NDVI composites were generated from daily data. Pixels with scan angles of less than 42° were preferentially selected in the compositing to reduce the effects of surface anisotropy. Both the daily and composite data have only pixels whose solar zenith angle was less than 80°.
- The global 8-km data set, is in the Interrupted Goode Homolosine equal area projection (Steinwand, 1994), and has an image size of 5004 pixels by 2168 scan lines for the entire globe.
- A lower resolution global NDVI data set in the Plate Carée projection, with 1° latitude by 1° longitude bins, also has been generated for the climate modeling community by spatially averaging the 8-km reflectance and brightness temperature data. NDVI for the 1° data set is recomputed from the average reflectances.
- To date, there are about 4800 daily images and 480 composite images stored in the DAAC, near-on-line, tape archive. Subsampled, lower volume browse data sets facilitate previewing the image data when ordering. The data is in HDF format (NCSA, 1990).
- A subset of the PAL parameters (composites only) for the period of 1981-1994 is stored on-line in flat binary format for ease of user access, and is available via FTP or a Web browser such as Netscape. This subset consists of channel 1 and 2 reflectances, derived NDVI, and blackbody brightness temperatures for channels 4 and 5.

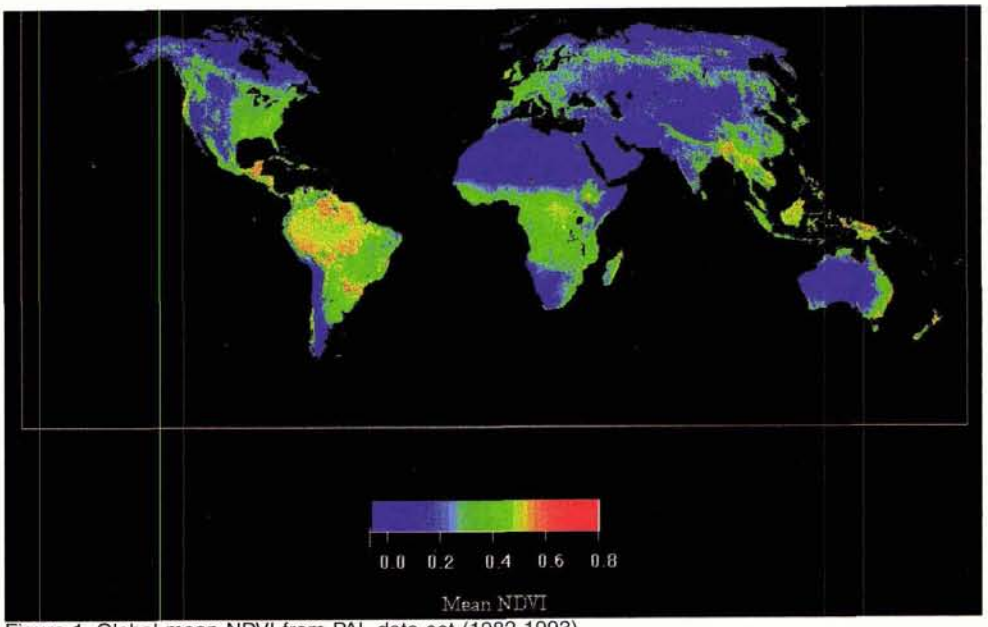

Figure 1. Global mean NDVI from PAL data set (1982-1993).

## Known problems with current data set

Three problems were discovered with the current data set. First, the visible and near-IR reflectances were not normalized for the variations in the solar zenith angle (sza). Second, an incomplete atmospheric correction had been applied. Third, there was an error in the computation of the sza, due to a software coding error that caused the sza error to be seasonally dependent and increase in magnitude with increasing time from the reference year 2000. The maximum sza error was ±7.5° for the earliest data year (1981). Post-processing code has been developed to remove this error, and test results indicate that the revised sza is usually within ± 0.2° of its correct value.

An analysis of the impact of these three errors on the NDVI and reflectance parameters showed that, when the corrected sza was used for normalization and a complete atmospheric correction applied, a typical NDVI value was changed from its uncorrected value by 0.02 NDVI units, while channels 1 and 2 reflectances were changed by about 2% and 3%, respectively.

GSFC's DAAC is reprocessing the original data set to remove these three errors and intends to reissue a corrected data set. Ten-day composite data will be corrected first and should be available by December, 1996, along with a CD-ROM product (one diskette per data year for the parameters stored on the FTP data set). Corrected daily images will be available by September, 1997.

## Potential applications

Due to its high information content, the PAL data set can be used for a variety of land science applications: land cover classification, monitoring desertification, Net Primary Production (NPP), assessing crop conditions, and the deriving of land surface parameters for climate modeling.

### Global vegetation dynamics

Although seasonal vegetation dynamics at

*Continued on page 27*

# Highlight

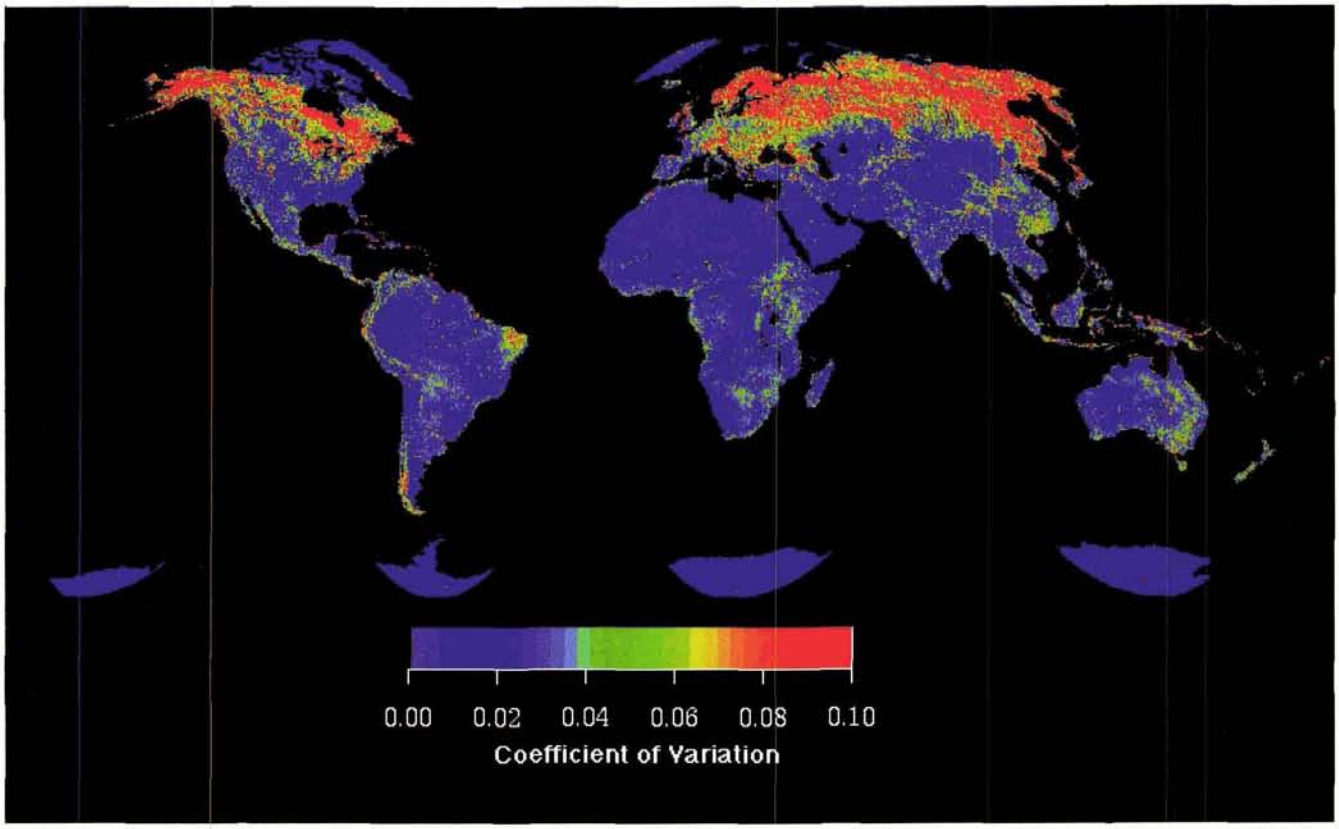


Figure 2. Interannual coefficient of variation of NDVI from PAL data set (1982-1993).

*Continued from page 13*
continental scales have been previously studied (i. e. Justice *et al.*, 1985), the changes between years, at a global scale, are not so well understood. Tucker *et al.* (1991) used the coefficient of variation of the mean growing season NDVI as a statistic to highlight vegetation changes over the Sahel region in Africa.

Figures 1 and 2 show the mean, and the coefficient of variation derived from the PAL monthly maximum value composites of NDVI for the time period 1982-1993. The coefficient of variation is computed for each pixel and highlights areas with maximum inter-annual variability. For the 1982-1993 data time period used in the study, the coefficient is defined as:

$$\frac{\textit{Standard deviation of 12 annual NDVI means}}{\textit{Mean NDVI for 12-year data period}}$$

Figure 2 shows, for the first time to our knowledge, the global coefficient of inter-annual variation of NDVI for a 12-year period for almost the entire Earth's terrestrial surface. Although similar products for Africa (e.g. Goward and Prince, 1995) and some related analyses (e.g. Myneni *et al.*, 1996) have been carried out, the PAL data set is ideal for globally comprehensive studies. A complete analysis of this image requires significant effort; however, some of the issues to be addressed in such an analysis are noted below. Bearing in mind that the data have a resolution of 8-km globally, it is clear that there is a great deal of information in the PAL data.

The most surprising feature of the global coefficient of variation image is the large area of high values in the northern temperate and boreal regions of Canada, Scandinavia, Europe, and Asia. Hot spots occur in eastern Brazil, tropical Africa, China, and Australia. The analysis of these signals should consider not only inter-annual variations in the vegetation, but also surface variations, such as snow cover and atmospheric changes caused by volcanic dust, as well as variations in the satellite platform itself, caused, for example, by orbital precession and hence solar zenith angle variation between years.

In the tropics, solar zenith angle and snow are not major factors and the NDVI is most likely to be affected by inter-annual variations in climatic, ecological, and human factors. Precipitation changes associated with El Niño southern oscillation events have been invoked to explain variations in NDVI in eastern Brazil, Africa, and Australia. The variability in the areas affected by winter precipitation (Cape Province, South Africa, Chile, Western Australia, California, Morocco) may be a result of variability in the latitudinal circulation cells resulting in greater or lesser influence of winter westerlies. At a finer scale, forest burning, grazing and agriculture can be expected to contribute variation.

These and other factors will have to be examined to account for the variability in the Earth's NDVI signal between years. In so far as it can be shown that these effects are real surface changes, and not

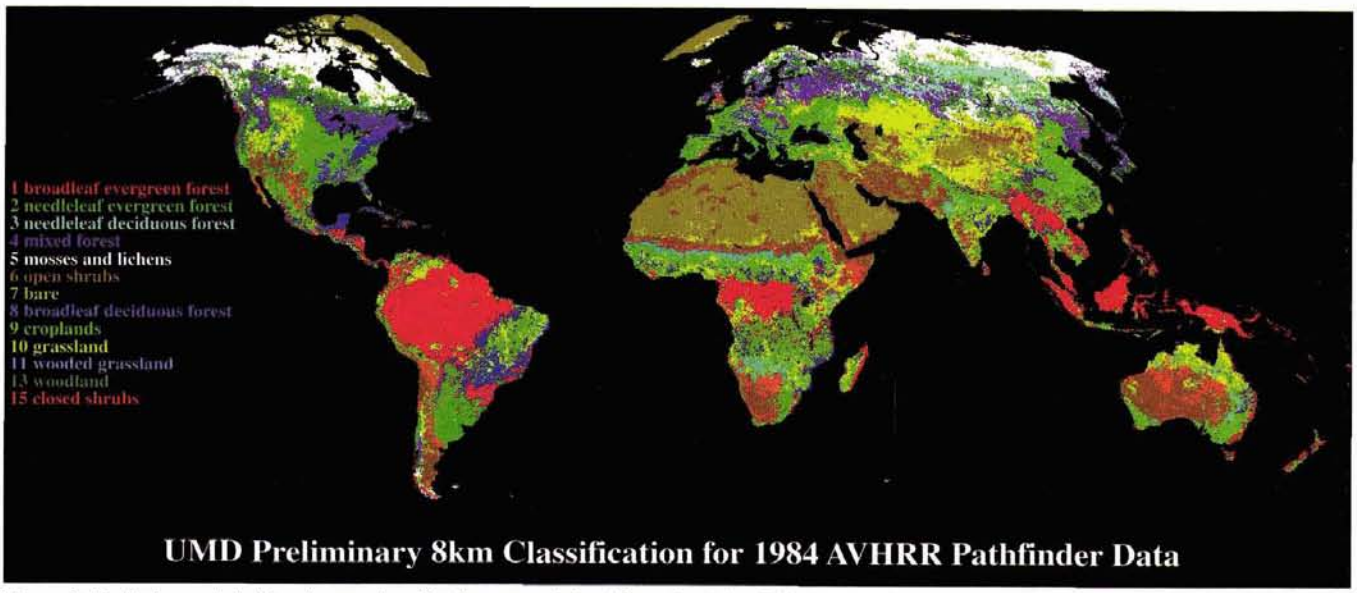


Figure 3. Preliminary global landcover classification map derived from the 8-km PAL data set for 1984.

artifacts of the platform and measurement system, we are faced with the possibility that the Earth as a whole varies significantly in important functional processes between years. NDVI is shown to be related to several critical Earth processes. The PAL data set enables these to be explored in a manageable data set for the first time.

### Global land cover classification using the PAL data

Numerous experiments investigating effects of changes in land cover on climate found significant effects on surface temperature, evapotranspiration, and precipitation (Lean and Warrilow, 1989; Shukla *et al.*, 1990; Keller *et al.*, 1991; Xue and Shukla, 1991; Bonan *et al.*, 1992). Thus, an accurate global land cover map is an important requirement for models that predict exchanges of water, energy and momentum from the biosphere to the atmosphere. Furthermore, accurate descriptions of the distribution of vegetation over the Earth's land surface are required for biogeochemical and atmospheric chemistry models as well as for natural resource management (Townshend, 1992).

Existing data sets of global land cover compiled from ground-based sources have a number of inaccuracies. These data sets were aggregated from local studies collected at different times and based on varying definitions of land cover type. Data reliability is an additional limitation: Such ground-based global data sets are known to be inaccurate and there is considerable disagreement among them on the spatial distribution of land cover types (Townshend *et al.*, 1991; DeFries and Townshend, 1994a). Consequently, researchers have turned to remotely sensed data to provide internally consistent and more accurate maps of global land cover.

Phenologies of different vegetation types, as reflected in intra-annual variations in the NDVI, provide a basis for mapping global and regional land cover. Tucker *et al.* (1985a) used NOAA's GVI to produce a general land cover classification for Africa, at a spatial resolution of 15 to 20 km, based on mean annual NDVI and seasonality. Townshend *et al.* (1987) classified land cover for South America using multiple images from different dates throughout the year. In addition, Loveland *et al.* (1991) used AVHRR local area coverage data at approximately 1-km spatial resolution for an unsupervised classification, which derived homogeneous land cover regions for the coterminous U.S., and currently are applying this methodology at a global scale. DeFries and Townshend (1994b, 1995) produced a global distribution of major land cover types based on a global 1° x 1° NDVI data set (Los *et al.*, 1994).

Currently, studies are underway to develop methodologies to map global land cover from the PAL data. The methodologies use all spectral bands and rely on decision tree methods to classify cover types (Hansen *et al.*, 1996). Based on a network of global training sites derived from high resolution Landsat data, a preliminary global land cover map was derived using the 1984 PAL data (Figure 3).

In addition to mapping thematic land cover types, PAL data is being used to determine subpixel proportions of vegetation characteristics that could provide more realistic descriptions of the land surface (DeFries *et al.*, 1995b). One such method involves linear mixture modeling to determine proportions in each pixel of woody vegetation, herbaceous vegetation, and bare ground and empirical estimation of land cover (DeFries *et al.*, 1996). An alternative method is based on empirical relationships between the percent forest cover derived from high resolution data and metrics derived from the PAL data (DeFries *et al.*, in press).

### Net primary production modeling

Global net primary production (NPP) describes the accumulation of carbon in the biosphere, and is an important com-

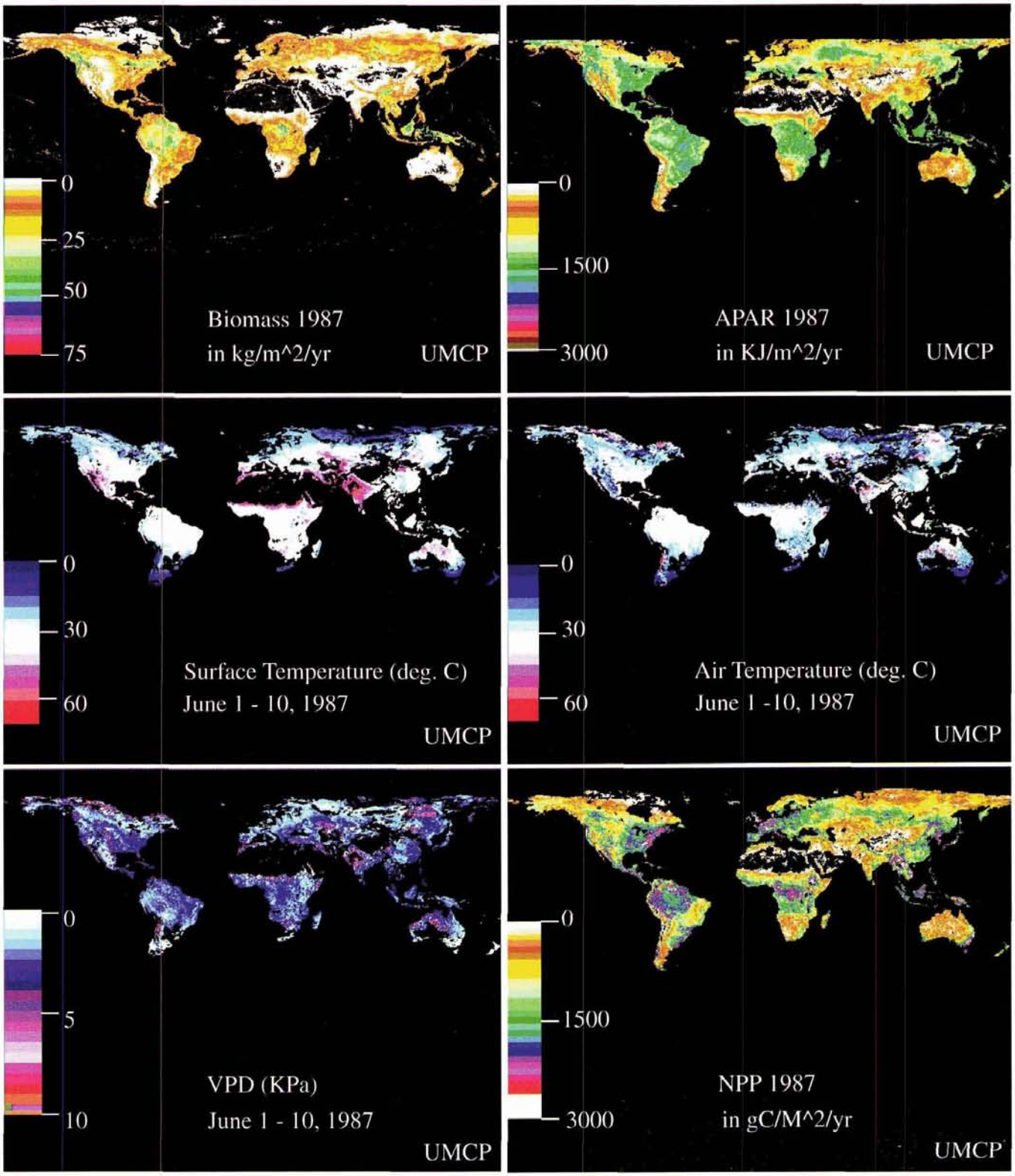


Figure 4. GLO-PEM model results for 1987. The output has been resampled to display 8 x 8 km results. (a) Biomass for year, (b) absorbed photosynthetically active radiation for year (APAR), (c) surface temperature (June 1 -10), (d) air temperature (June 1-10), (e) vapor pressure deficit (June 1-10), and (f) net primary production for year. Thes images indicate the wide variety of ecosystems variables that are inferred from satellite data by GLO-PEM.

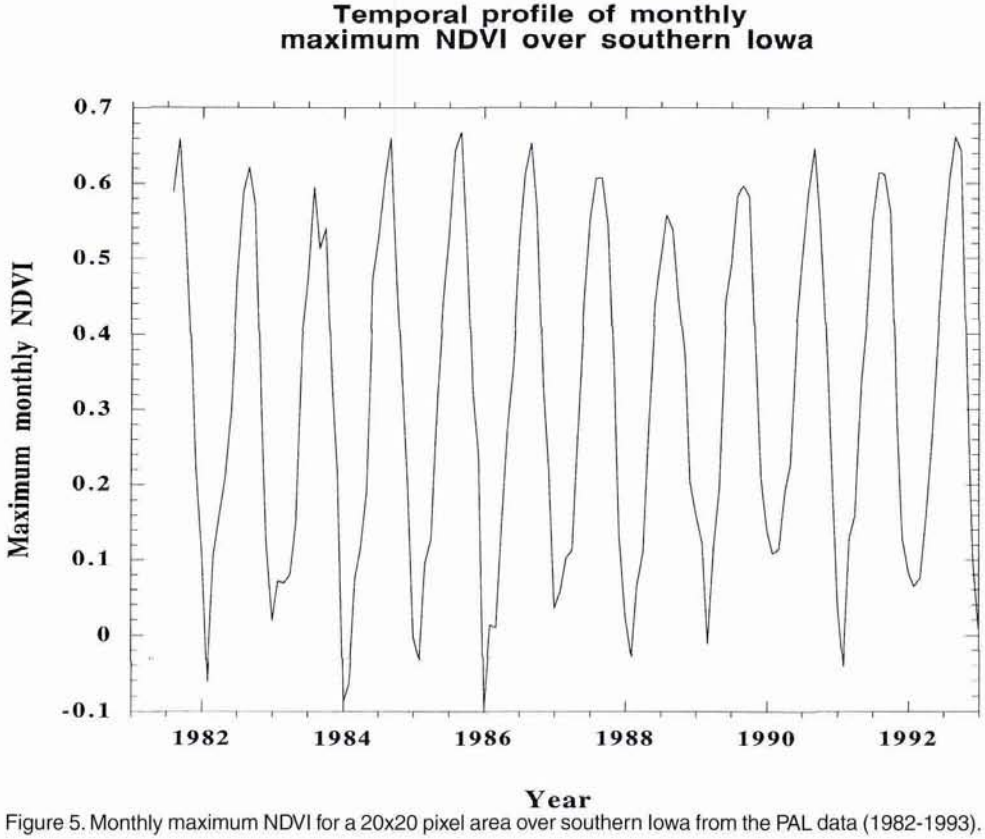


Figure 5. Monthly maximum NDVI for a 20x20 pixel area over southern Iowa from the PAL data (1982-1993).

ponent of the carbon chain in the environment (Field *et al.*, 1995). Global AVHRR data sets have been previously used in NPP models of various types (Potter *et al.*, 1993; Ruimy *et al.*, 1996). Initially, AVHRR NDVI data were summed throughout the growing season and the total was related to productivity using empirical, regression models (Prince, 1991b, Tucker *et al.*, 1985b). More mechanistic models have since been devised, inspired by a crop model proposed by Kumar and Monteith (1982) and Prince (1991a).

Global Production Efficiency Model (GLO-PEM) is a mechanistic primary production model to study global ecological processes. The basis of the model is the production efficiency approach in which the NPP is estimated from the amount of photosynthetically active radiation (PAR) absorbed by the plant canopy (APAR) and an efficiency of conversion of this energy into biomass (Prince, 1991; Prince and Goward, 1995). It differs from other global models in several important respects, most important is the use of satellite data for all model forcing variables; no climate data or climatologies or field NPP calibration steps are used. Several innovative algorithms are implemented in GLO-PEM that are used to compute a variety of forcing variables such as surface temperature, air temperature, atmospheric precipitable water, vapor pressure deficit, soil moisture stress, and aboveground biomass from the satellite data. In the present implementation, the 8x8 km resolution, 10-day composite PAL data are used to compute these variables. The PAL data set is ideal for GLO-PEM, since it is the only AVHRR data set that is able to provide the individual channel data in a consistent form for the full observation period.

Figure 4 shows some model results for 1987. Satellite data alone are used because of their unique advantages of repetitive, continuous, time-specific observations; the measurement of actual rather than potential vegetation cover; and their global coverage with spatially contiguous observations.

## Crop monitoring

In order to make an accurate assessment of crop condition and yield, agricultural forecasts should have the qualities of objectivity, reliability, timeliness, adequacy of coverage, efficiency, and effectiveness (MacDonald and Hall, 1980). Over the years, a great deal of experience has been acquired in collecting, analyzing and interpreting data from agricultural field trials of arable crops (Clevers, 1986). The traditional method of acquiring quantitative data in the field is by multiple sampling. Such an approach is both labor intensive and time consuming. At regional scales, the only appropriate instruments for developing a continuous database are satellite-based sensors (Price, 1989).

In dynamic agricultural growth models, the state of the system at any time is determined by a set of driving or forcing variables such as evapotranspiration (ET) and APAR. Research in remote sensing for agricultural studies mainly has focused on crop yield forecasting and dry matter accumulation (Tucker *et al.*, 1980; Kumar and Monteith, 1982; Aase *et al.*, 1984; Maas, 1988; Doraiswamy and Cook, 1995), on measuring agronomic and agroclimatic parameters such as ET and APAR (Price, 1990; Daughtry *et al.*, 1992), on the evaluation of stress due to water and pest infestation (Jackson and Ezra, 1985; Hatfield *et al.*, 1985), and on measuring harvest indices and estimating crop acreage (Badhwar, 1984; Rudorff and Batista, 1991). Vegetation indices such as NDVI also have been widely used to determine the temporal changes in crop growth (e.g., Wiegand and Richardson, 1990; Bennedetti and Rossini, 1993). Sellers (1985, 1987) has shown that vegetation indices can also be used

to measure the rate variables of the vegetation systems such as photosynthesis and stomatal conductance. The National Agricultural Statistics Service (NASS) of the U.S. Department of Agriculture (USDA) uses NDVI from AVHRR as one of the variables to monitor agricultural conditions at the county, agricultural statistics district, and state levels (Doraiswamy and Cook, 1995). Most of these studies were conducted over small geographic regions using high resolution AVHRR Local Area Coverage (LAC) data, which has a nominal spatial resolution of 1 km. However, for practical reasons, when crop condition assessment has to be performed at a global scale, a coarse resolution data set is needed.

The PAL data set provides a continuous long-time record of multi-spectral measurements thus offering unique opportunity to study the relationships between satellite measurements and crop conditions. Figure 5 shows the temporal profile of mean NDVI over a 20x20 pixel area in an agricultural region of southern Iowa over a 12-year period. Peaks in the sinusoidal profile coincide with the maximum photosynthetic activity in a given year's growing season. The 1988 growing and harvest season is the driest on record. The significantly lower levels of NDVI during the summer of 1988 correspond to one of the worst droughts of the century in this region (Teng, 1990).

## Data access

Users may obtain AVHRR data products and documentation describing these products from the Goddard DAAC.

NASA/GSFC, code 902
Goddard DAAC
Greenbelt Road
Greenbelt MD 20771

Electronic access is available through the Web or FTP.

WWW access:
http://daac. gsfc. nasa. gov/CAMPAIGN_DOCS/LAND_BIO/GLBDST_main.hmtl

FTP access:
ftp daac. gsfc. nasa. gov
login as anonymous, at the password prompt enter your email address, cd data/avhrr.

A user help desk is available to assist users with problems: 301-614-5224 or 800-257-6151, fax 301-614-5268).

## Summary

The PAL data is a valuable resource to the land science community. It was produced with an invariant algorithm and was carefully validated. It covers a long time period (1981-1994) and is available at 8 km and 1°x1° spatial resolutions.

Some of the potential applications of this data set are global vegetation dynamics studies, crop monitoring, and NPP modeling. The long time period of the PAL data set permits the exploration of inter-annual variability in response to El Niño and other climatic fluctuations.

For land cover studies, 1°x1° resolution data obscure much of the heterogeneity of the land surface. The 8 km resolution of the PAL data set provides the basis to capture much of this heterogeneity. While previous global land cover classification approaches relied mostly on NDVI (DeFries and Townshend, 1994b), land cover discrimination could be significantly improved when the reflectances and brightness temperatures from the individual AVHRR channels are incorporated into the classification algorithm (DeFries *et al.*, 1995a). Also, the individual channel information from the continuous, long-term record could be used to derive the ecosystem variables required to model annual global NPP using physically based models.

For the climate modeling community, the long temporal period of this data set, which immediately precedes the upcoming EOS mission, makes PAL an important, precursor data set for the Moderate-Resolution Imaging Spectroradiometer (MODIS) experiment to be flown on the EOS am platform (Asrar and Greenstone, 1995).

## Acknowledgements

Generation of the PAL data set was funded by the NASA's Mission to Planet Earth Office, Pathfinder program. Partial funding for this research was from NASA grants NAG52396 (PAL data set validation) and NAGW4206 (landcover analysis). The support of Martha Maiden (NASA), John Townshend (Univ. of Maryland, Geography Dept. ), and Mary E. James (formally of NASA) is gratefully acknowledged. The authors wish to thank Matthew Hansen (Univ. of Maryland, Geography Dept.) for analysis support for the generation of the landcover classification map and William Teng (Hughes STX Corp., GSFC) for reviewing and critiquing this article. Bob Rank, Andy Griffin, Bin-bin Ding, Dana Kerr, Angela Hewitt, and John Bonk were responsible for operations and software support for the PAL data set.

## About the Authors

[1] Code 902, NASA-GSFC, Greenbelt, MD 20771
psmith@wind.gsfc.nasa.gov

[2] Dept. of Geography, University of Maryland at College Park, College Park, MD 20742

## References

Aase, J.K., F.H. Siddoway, and J.P. Millard, 1984. Spring wheat—leaf phytomass and yield estimates from airborne scanner and hand held radiometer measurements. *International Journal of Remote Sensing*, 5:771-778.

Asrar, G., and R. Greenstone, eds., 1995. *Mission to Planet Earth 1995/MTPE/EOS Reference Handbook*.

Badhwar, G.D., 1984. Classification of corn and soybeans using multitemporal thematic mapper data. *Remote Sensing of Environment*, 16:175-182.

Baldwin, D., and W.J. Emery, 1993. Systematized approach to AVHRR navigation, *Annals of Glaciology*, 17:414-420.

Bennedetti, R., and P. Rossini, 1993. On the use of NDVI profiles as a toll for agricultural statistics: The case study of wheat yield estimate and forecast in Emilia Romagna, *Remote Sensing of Environment*, 45:311-326.

Bonan, G.B., D. Pollard, and S.L. Thompson, 1992. Effects of boreal forest vegetation on global climate, *Nature*, 359:716-717.

Clevers, J.G.P.W., 1986. Applications of remote sensing to agricultural field trials, Agricultural university, Paper No.86-4 (The Netherlands: Wagningen).

Daughtry, C.S.T., K.P. Gallo, S.N. Goward, S.D. Prince, and W.P. Kustas, 1992.Spectral estimates of absorbed radiation and phytomass production in corn and soybean canopies.*Remote Sensing of Environment*, 39: 141-152.

DeFries, R.S., C.B. Field, F. Inez, C.O. Justice, P.A. Matson, M. Matthews, H.A. Mooney, C.S. Potter, K. Prentice, P.J. Sellers, J.R.G. Townshend, C.J. Tucker, S.L. Ustin, and P.M. Vitousek, 1995a. Mapping the land surface for global atmosphere-biosphere models: toward continuous distributions

of vegetation's functional properties, *Journal of Geophysical Research*, 100, (D10), 20:867-20,882.

DeFries, R.S., M. Hansen, M. Steininger, R. Dubayah, R. Sohlberg, and J.R.G. Townshend. Subpixel forest cover in Central Africa from multisensor, multitemporal data, *Remote Sensing of Environment*. (In Press)

DeFries, R.S., M. Hansen, and J.R.G. Townshend, 1995b. Global discrimination of land cover types from metrics derived from AVHRR Pathfinder data, *Remote Sensing of Environment*, 54: 209-222.

DeFries, R., M. Hansen, and J.R.G. Townshend, 1996. Proportional estimation of land cover characteristics from satellite data, *International Geoscience and Remote Sensing Symposium*, Lincoln, Nebraska, pp.

DeFries, R.S., and J.R.G. Townshend, 1994a. Global land cover: comparison of ground-based data sets to classifications with AVHRR data. In *Environmental Remote Sensing from Regional to Global Scales*, G. Foody and P. Curran, eds. Environmental Remote Sensing from Regional to Global Scales, (U.K.: John Wiley and Sons).

DeFries, R.S., and J.R.G. Townshend, 1994b. NDVI-derived land cover classification at global scales, *International Journal of Remote Sensing*, 15(17):3567-3586.

DeFries, R.S., and J.R.G. Townshend, 1995. An initial coarse resolution NDVI-derived global land cover classification, in *ISLSCP Initiative I—Global Data Sets for Land-Atmosphere Models*, 1987-1988. Vols. 1-5, B.W. Meeson, F.E. Corprew, J.M.P. McManus, D.W. Myers, J.W. Closs, K.-J. Sun, D.J. Sunday, and P.J. Sellers, eds. Published on CDROM by NASA (USA_NASA_GDAAC_ISLSCP_001-USA_NASA_GDAAC_ISLSCP_005).

Doraiswamy, P.C., and P.W. Cook, 1995. Spring wheat yield assessment using NOAA AVHRR data. *Canadian Journal of Remote Sensing*, 21:43-51.

Field, C.B., J.T. Randerson, and C.M. Malmström, 1995. Global net primary production: combining ecology and remote sensing, *Remote Sensing of Environment*, 51(1):74-88.

Gordon, H.R., J.W. Brown, and R.H. Evans, 1988. Exact Rayleigh scattering calculations for use with the Nimbus-7 Coastal Zone Color Scanner, *Applied Optics*, 27:862-870.

Goward, S.N., and S.D. Prince, 1995. Transient effects of climate on vegetation dynamics: satellite observations, *Journal of Biogeography*, 22:549-563.

Goward, S.N., R.H. Waring, D.G. Dye, and Yang, J., 1994. Ecological remote sensing at OTTER: satellite macroscale observations, *Ecological Applications*, 42(2):322-343.

Hansen, M., R. Dubayah, and R.S. DeFries, 1996. Classification trees: An alternative to traditional land cover classifiers, *International Journal of Remote Sensing*, 17(5):1075-1081.

Hatfield, J.L., D.F. Wanjura, and G.L. Barker, 1985, Canopy temperature response to water stress under partial canopy, *Transactions of the ASAE*, 28:1607-1611.

Jackson, R.D., and C.E. Ezra, 1985. Spectral response of cotton to suddenly induced water stress, *International Journal of Remote Sensing*, 6:177-185.

James, M.E., and S.N.V. Kalluri, 1994. The Pathfinder AVHRR land data set: an improved coarse resolution data set for terrestrial monitoring, *International Journal of Remote Sensing*, 15:3347-3363.

Justice, C.O., J.R.G. Townshend, B.N. Holben, and C.J. Tucker, 1985. Analysis of the phenology of global vegetation using meteorological satellite data, *International Journal of Remote Sensing* , 6:1271-1381.

Keller, M.D., D.J. Jacob, S.C. Wofsy, and R.C. Harris, 1991. Effects of tropical deforestation on global and regional atmospheric chemistry, *Climate Change*, 19:139-158.

Kidwell, K.B., 1991. NOAA Polar Orbiter Data User's Guide (Wash. D.C.: NOAA/NCDC/SDSD, National Climate Data Center).

Kumar, M., and J.L. Monteith, 1982. Remote sensing of plant growth. Pages 133-144 in H. Smith, ed. *Plants and the Daylight Spectrum*, Academic Press, London.

Lean, J., and D.A. Warrilow, 1989. Simulation of the regional climatic impact of Amazon deforestation, *Nature*, 342:411-413.

Los, S.O., C.O. Justice, and C.J. Tucker, 1994. A global 1 x 1 degree NDVI data set for climate studies derived from the GIMMS continental NDVI data, *International Journal of Remote Sensing*, 15(17):3493-3518.

Loveland, T.R., J.W. Merchant, D.O. Ohlen, and J.F. Brown, 1991. Development of a land-cover characteristics database for the coterminous U.S., *PE&RS*, 57(11):1453-1463.

Maas, S.J., 1988. Use of remotely-sensed information in agricultural crop growth models, *Ecological Modeling*, 41:247-268.

MacDonald, R.B., and F.G. Hall, 1980. Global crop forecasting, *Science*, 208:670-679.

Myneni, R.B., S.O. Los, and C.J. Tucker, 1996. Satellite-based identification of linked vegetation index and sea surface temperature anomaly areas from 1982-1990 for Africa, Australia and South America, *Geophysical Research Letters*, 23:729-732.

NCSA, 1990. Hierarchical Data Format (HDF) User's Guide, National Center for Supercomputing Applications, University of Illinois at Urbana-Champaign, Urbana-Champaign, Illinois.

Patt, F.S., and W. Gregg, 1994. Exact closed-form geolocation algorithm for Earth survey sensors, *International Journal of Remote Sensing*, 15:3719-3734.

Potter, C.S., J.T. Randerson, C.B. Field, P.A. Matson, P.M. Vitousek, H.A. Mooney, and S.A. Klooster, 1993. Terrestrial ecosystem production: a process model based on global satellite and surface data, *Global Biogeochemical Cycles*, 7:811-841.

Price, 1989. Quantitative aspects of remote sensing in the thermal infrared. In *Theory and Applications of Optical Remote Sensing*, edited by G. Asrar, pp. 578-603 (New York: John Wiley & Sons).

Price, J.C., 1990. Using spatial context in satellite data to infer regional scale evapotranspiration. *IEEE Trans. Geos. and Remote Sensing*, GE28:940-948.

Prince, S.D., 1991a. A model of regional primary production for use with coarse-resolution satellite data, *International Journal of Remote Sensing*, 12:1313-1330.

Prince, S.D., 1991b. Satellite remote sensing of primary production:comparison of results for Sahelian grasslands 1981-1988. *International Journal of Remote Sensing*, 12:1301-1311.

Prince, S.D., and S.N. Goward, 1995. Global primary production: a remote sensing approach, *Journal of Biogeography*, 22:815-835.

Rao, C.R.N., 1993. Non-linearity corrections for the thermal infrared of the Advanced Very High Resolution Radiometer: assessment and recommendations, *NOAA Technical Report NESDIS-69*, NOAA/NESDIS, Washington D.C., Dept. of Commerce.

Rao, C.R.N., and J. Chen, 1994. Post launch calibration of the visible and near infrared channels of the advanced very high resolution radiometer on NOAA-7, -9, and -11 spacecraft, *NOAA technical report NESDIS-78*, Washington DC, Dept. of Commerce.

Rudorff, B.F.T., and G.T. Batista, 1991, Wheat yield estimation at the farm level using TM Landsat and agrometeorological data. *International Journal of Remote Sensing*, 12:2477-2484.

Ruimy, A., G. Dedieu, and B. Saugier, 1996. TURC: a diagnostic model of continental gross primary productivity and net primary productivity, *Global Biogeochemical Cycles*, 10: 269-285.

Sellers, P.J., 1985. Canopy reflectance, photosynthesis, and transpiration, *International Journal of Remote Sensing*, 6:1335-1371.

Sellers, P.J., 1987. Canopy reflectance, photosynthesis, and transpiration, II. The role of biophysics in the linearity of their interdependence, *Remote Sensing of Environment*, 21:143-183.

Shukla, J., C. Nobre, and P. Sellers, 1990. Amazon deforestation and climate change, *Science*, 247:1322-1325.

Steinwand, D.R., 1994. Mapping raster imagery to the Interrupted Goode Homolosine projection, *International Journal of Remote Sensing*, 15:3463-3471.

Stowe, L.L., E.P. McClain, P. Pellegrino, G. Gutman, P. Davis, C. Long, and S. Hart, 1991. Global distribution of cloud cover derived from the NOAA/AVHRR operational satellite data, *Advances in Space Research*, 3:51-54.

Teng, W.L., 1990. AVHRR monitoring of U.S. crops during the 1988 drought, *Photogrammetric Engineeering and Remote Sensing*, 56:8:1143-1146.

Townshend, J.R.G., ed., 1992. Improved Global Data for Land Applications: A Proposal for a New High Resolution Data Set, *Report No. 20, (Stockholm, Sweden: International Geosphere-Biosphere Programme)*.

Townshend, J.R.G., 1994. Global data sets for land applications from the Advanced Very High Resolution Radiometer: an introduction, *International Journal of Remote Sensing*, 15:3319-3332.

Townshend, J.R.G., C.O. Justice, and V.T. Kalb, 1987. Characterization and classification of South American land cover types using satellite data, *International Journal of Remote Sensing*, 8:1189-1207.

Townshend, J.R.G., C.O. Justice, W. Li, C. Gurney, and J. McManus, 1991. Global land cover classification by remote sensing: present capabilities and future possibilities, *Remote Sensing of the Environment*, 35:243-256.

Tucker, C.J., H.E. Dregne, and W.W. Newcomb, 1991. Expansion and Contraction of the Sahara desert from 1980 to 1990, *Science*, 253:299-301.

Tucker, C.J., B.N. Holben, J.H. Elgin, and J.E. McMurtrey, 1980. Relationship of spectral data to grain yield variation, *PE&RS*, 46:657-666.

Tucker, C.J., J.R.G. Townshend, and T.E. Goff, 1985a. African land-cover classification using satellite data, *Science*, 227: 369-375.

Tucker, C.J., C.L. Vanpraet, M.J. Sharman, and G. Van Ittersum, 1985b. Satellite remote sensing of total herbaceous biomass production in the Senegalese Sahel: 1980-1984, *Remote Sensing of the Environment*, 17:233-249.

Wiegand, C.L. and A.J. Richardson, 1990. Use of spectral vegetation indices to infer leaf area, evapotranspiration, and yields: II. Results, *Agronomy Journal*, 82: 630-636.

Xue, Y., and J. Shukla, 1991. The influence of land properties on Sahel climate Part 1: desertification, *Journal of Climate*, 6:2232-2245.